Cooling Gas Comparison and Influence of Flow Conditions for Film Cooling in Laminar and Turbulent Supersonic Flow

M. Hombsch and H. Olivier
Shock Wave Laboratory, RWTH Aachen University
Templergraben 55, 52056 Aachen

Abstract

In the scope of a film cooling analysis for future rocket nozzles, experiments with cooling gas injection into laminar and turbulent flat plate flow have been conducted at the Shock Wave Laboratory RWTH Aachen University. Laminar film cooling with an injection slot was investigated at different blowing ratios, Mach numbers and with different cooling gases. For turbulent film cooling, blowing holes and slotted injection were studied, changing the blowing ratio and the Mach number as well. Cooling efficiencies were deduced from heat flux data, and were correlated with a correlation function.

1. Introduction

Numerical simulations of rocket nozzle cooling by tangential blowing have been investigated by Martelli et al. for turbulent flow [1]. They proposed a correlation of the cooling behavior dependant of the distance to the blowing opening, the slot height, the blowing ratio and the ratio of constant pressure specific heats. When looking at the formula used, the blowing ratio F and the slot height s appear as a product, representing the mass flow Fs as important parameter. Although with different free stream conditions and accelerated flow, correlated cooling efficiencies seem to match well with the flat plate experiments of this work, as discussed in chapters 2 and 4. Experimental investigations were conducted by Keener et al. [2], investigating transpiration cooling in a 2-D Mach 2 nozzle attached to a shock tube. Their findings were that the boundary layer thickness has major effect on the wall heat fluxes. Transpiration of coolant through a porous section of the wall leads to thickening of the boundary layer and a decrease of the heat fluxes. On the other hand, high heat fluxes are reached when the flow starts with the nozzle shock, where no boundary layer is present. Keener et al. also observed higher heat fluxes for suction, decreasing the boundary layer thickness. Yang et al. investigated laminar hypersonic film cooling numerically [3] and compared the results with experimental data from Richards [4]. A low total temperature and static pressure of the main flow leads, to their opinion, to low heat fluxes. The total temperature is incorporated via the recovery temperature in the definition of the cooling efficiency, describing this effect. The static pressure is proportional to the static density of the main flow, when flow at the same temperature is regarded. With the Reynolds number being part of the correlation parameter used here, this effect is described as well. Furthermore, Yang et al. reported increased cooling with an increasing mass flow of the coolant, with the slot height being unimportant. This complies with the results presented in this paper as the cooling efficiency scales with the mass flow Fs rather than with the blowing ratio F or the slot width s alone. In contrast to most available experimental data film cooling in rocket engines takes place with water vapor as main flow and a coolant film of either either hydrogen or water vapour as well, as in the research by Martelli et al. proposing fuel pump engine exhaust gas for film cooling [1]. To be able to transfer the knowledge based on experiments with both gases being air to the case of rocket engines, the influence of different coolant and main stream gases has to be known. Therefore a testing campaign has been conducted using four different cooling gases with air as main flow. Furthermore the flow inside a rocket nozzle is accelerated and thus covers a wide range of Mach numbers and Reynolds numbers, so cooling efficiency data was obtained for different flow conditions. The flow conditions were altered by changing the angle of attack of a flat plate model with the leading edge shock reducing the flat plate Mach number to the desired value. Investigated were Mach numbers of 1.5, 2.6, and 4.9 with the corresponding Reynolds numbers of 3.0, 4.9 and 6.3 mio/m.

2. Theoretical basis

Investigations concerning film cooling commonly refer to the non-dimensional cooling efficiency. It describes the ratio of surface temperature decrease due to cooling and the maximum temperature difference possible, Eq. (1). The temperature decrease the coolant achieves is expressed by subtracting the adiabatic wall temperature with cooling $T_{aw,c}$ from the recovery temperature T_r representing the adiabatic state without cooling. Maximum cooling is achieved, when the wall reaches the reservoir temperature of the cooling gas $T_{c,0}$. In the latter case both subtractions will be equal and their fraction unity.

$$\eta = \frac{T_r - T_{aw,c}}{T_r - T_{c,0}} \tag{1}$$

This expression for the cooling efficiency can be transferred to an expression for isothermal conditions, measuring the wall heat fluxes [5]. Thus, experiments with very short measuring time of a few milliseconds can be used to obtain cooling efficiency data. The ratio of heat transfer coefficients λ_{nc}/λ_c can be approximated by unity, which is valid for most of the blowing ratios investigated with $F < 0.5$ [5, 6]. To correct small deviations of free stream conditions, Stanton numbers are used instead of heat fluxes.

$$\eta = 1 - \frac{\dot{q}_c \lambda_{nc}}{\dot{q}_{nc} \lambda_c} \approx 1 - \frac{\mathrm{St}_c}{\mathrm{St}_{nc}} \tag{2}$$

The cooling efficiency is influenced by parameters like the blowing ratio F, Eq. (3), the slot width s, the cooling gas density, the Mach number and the Reynolds number of the main flow.

$$F = \frac{\rho_c u_c}{\rho_e u_e} \tag{3}$$

In order to predict and compare cooling efficiencies Goldstein presented a correlation function for turbulent subsonic flow [6]. This correlation has been modified for turbulent compressible flow, Eq. (5), and for laminar compressible flow, Eq. (4) [7], according to the reference temperature method by Eckert [8] and Simeonides [9].

$$\eta_l = f(\xi_l); \qquad \text{with} \qquad \xi_l = \left(\frac{x}{x_{ref}}\right)^{0.5} \left(\frac{C^*}{\mathrm{Re}_u}\right)^{0.5} \frac{x'^{0.5}}{F s} \tag{4}$$

$$\eta_t = f(\xi_t); \qquad \text{with} \qquad \xi_t = \left(\frac{C^*}{\mathrm{Re}_u}\right)^{0.2} \left(\frac{T_e}{T^*}\right)^{0.6} \frac{x'^{0.8}}{F s} \tag{5}$$

This correlation shows dependencies of the cooling efficiency on several factors. First of all, it has to be mentioned, that $f(\xi)$ is a monotonic decreasing function, meaning that a high correlation parameter implies a low cooling efficiency. Thus, a large distance from the slot exit x' leads to a low cooling efficiency. A high cooling gas mass flux $F s$ increases the efficiency as it serves as denominator in ξ. A high unit Reynolds number Re_u has a positive influence on the cooling as well. For laminar flow, an empirical factor $(x/x_{ref})^{0.5}$ has been introduced by Heufer to account for the natural growth of the incoming boundary layer with $x_{ref} = x_{slot}^{1.16}$ and both values in meters [7]. If gases other than that of the main flow are used for cooling, an additional factor can be introduced, which leads to a correlation of experiments with different gas properties. The original equations from Goldstein [6] include a gas factor $c_{p,e}/c_{p,c} \cdot k_c/k_e$ to be multiplied to the correlation parameter ξ. This factor implies that gases with high heat capacity c_p and low thermal conductivity k serve as potent coolants. According to a previous work, [14], a different gas factor has been proposed for laminar flow. Instead of the heat capacity and thermal conductivity, gas exchange inbetween main flow and coolant due to diffusion is assumed, with a low diffusion coefficient $D_{1,2}$ leading to high cooling efficiencies. This has been observed by Sahoo previously when injecting into the stagnation point of a blunt nose in hypersonic flow [10]. Furthermore the coolant film thickness is believed to play a major role as mentioned by Keener et al. [2] and Gülhan and Braun [15], as it shields the wall from the outer flow, thus, the specific volume of the coolant is an important parameter. Numerical calculations show that a much thicker coolant film establishes, when helium is injected at the same mass

flow than e.g. air, leading to lower heat fluxes. A high viscosity μ has a similar effect, as it thickens the coolant layer as well. These effects combine to an additional cooling gas factor for the correlation function.

$$\eta = f(\xi^*); \qquad \xi^* = \xi \left(\frac{D_{1,2}\rho}{\mu}\right)_c \left(\frac{\mu}{D_{1,2}\rho}\right)_e \tag{6}$$

When plotted versus the correlation parameter, experimental results of different laminar film cooling experiments are quite similar to each other and can be expressed by one curve fit, Eq. (7). The same holds for turbulent flow, with another curve fit, Eq. (8). A similar correlation has been conducted by Martelli et al. for an analysis of supersonic injection in rocket nozzles, Eq. (9) [1]. In this case, tangential injection takes place in the first part of a dual bell nozzle in a turbulent Mach 3.65 main flow. The flow accellerates to a Mach number of 3.93 before entering the second bell. Values for the correlation parameter ξ_t are about 33 times higher than those for the correlation, Eq. (8). The reason for this are missing factors in the correlation function containing, for instance, the Reynolds number. More details on the results of Martelli et al. are given in section 4.

$$\eta_l = \begin{cases} 1 & \left|\xi_l \le 0.96\right. \\ [0.38\,(\xi_l - 0.96) + 1]^{-1,6} & \left|\xi_l > 0.96\right. \end{cases} \tag{7}$$

$$\eta_t = \begin{cases} 1 & \left|\xi_t \le 1.85\right. \\ [0.32\,(\xi_t - 1.85) + 1]^{-0.8} & \left|\xi_t > 1.85\right. \end{cases} \tag{8}$$

$$\xi_{M,t} = \left(\frac{c_{pe}}{c_{pc}}\right)\frac{x'}{Fs} \qquad \text{with} \qquad \eta_{M,t} = \begin{cases} 1 & \left|\xi_{M,t} \le 61\right. \\ [0.0164\xi_{M,t}]^{-0,38} & \left|\xi_{M,t} > 61\right. \end{cases} \tag{9}$$

3. Experimental setup

Experiments were conducted using different flat plate models mounted on a wedge carrier. The plate is inclined to the free stream with an adjustable angle and a leading edge shock establishes. This shock reduces the Mach number of the free stream from 8 to a flat plate flow of $Ma = 1.5$, 2.6 and 4.9. The inclination angles used to obtain these Mach numbers were 40°, 30° and 15°, respectively. Due to the change of the leading edge shock strength, different Mach numbers imply different densities and temperatures on the flat plate. Along with the temperature, the viscosity changes as well. These effects lead to a variation of the unit Reynolds number when changing the Mach number. Therefore the Mach numbers of $Ma = 1.5$, 2.6 and 4.9 come along with unit Reynolds numbers of 3.0, 4.9 and 6.3 millions/m. The flat plate is equipped with different injection slots or a set of blowing holes, all sharing the same length of 120 mm to ensure a two-dimensional cooling gas flow on the center-line of the model. Thermocouples are used to record surface heat flux changes due to cooling. For the laminar film cooling experiments, an injection slot of 0.5 mm width and an inclination of 45° to the flat-plate flow has been employed, see Fig. 1a). For experiments with turbulent boundary layer flow, a tripping device is necessary, therefore a strip of sandpaper is inserted close to the leading edge. Investigations were conducted with a blowing slot of small inclination angle of 10°, see Fig. 1b). Two rows of staggered blowing holes have been investigated as well, with the holes beeing inclined at 45° to the plate flow, see Fig. 1c)

The models are placed in the shock tunnel TH2, which provides a Mach 8 flow for a short duration of a few milliseconds. The flow reaches $T_0 = 1200$ K and $\mathrm{Re}_{u,\infty} = 2.6$ mio/m [11] [12] with the low enthalpy condition used. The facility consists of a classical shock tube with a nozzle attached, that ends in a vacuum chamber containing the model, see Fig. 2. The shock tube is driven by helium at 10 MPa in the high pressure section, separated from the low pressure section by membranes prior to the experiment. The incident shock from the high pressure section triggers the measuring equipment and reflects in front of the nozzle, compressing the test gas to the stagnation state of the nozzle flow, in this case 6 MPa. As described at the beginning of this chapter, the Mach 8 nozzle flow is deflected by the leading edge shock of the wedge model, leading to a lower Mach number for the flat plate flow. In order to guarantee a uniform flow for turbulent cooling experiments, infrared thermography was used to record the temperature distribution on the model surface during the experiments. As an example, Fig. 3 shows a picture of film cooling using two rows of blowing holes. At the leading edge a laminar boundary layer establishes which gets disturbed by a strip of
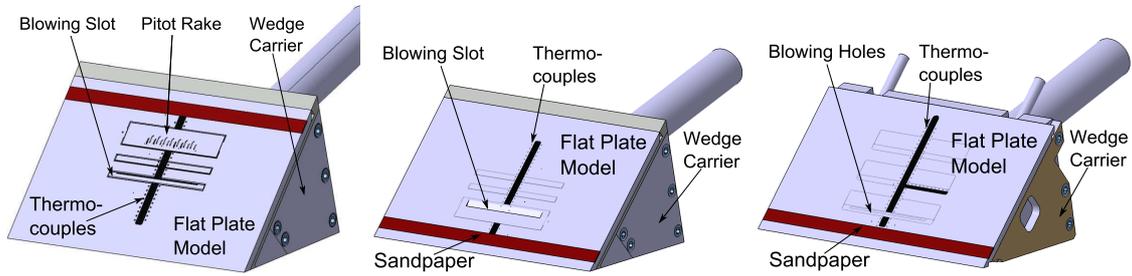
Figure 1: Wedge model with a) 45° slot blowing for laminar flow, b) 10° slot blowing for turbulent flow and c) two rows of 45° inclined blowing holes for turbulent flow.
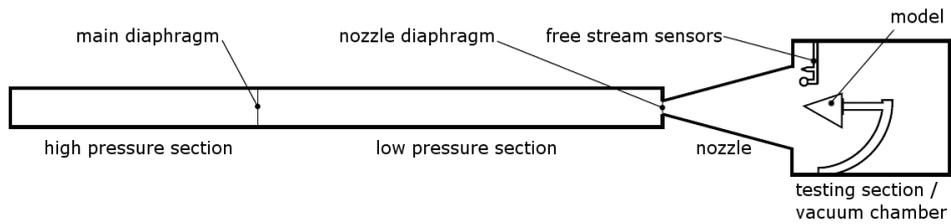

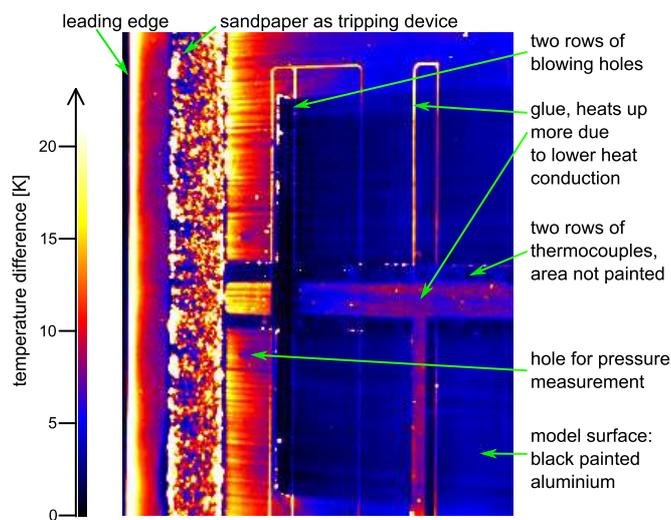Figure 2: Sketch of the Shock Tunnel TH2.

Figure 3: Infrared temperature image of the model with blowing holes in turbulent flow. $Ma_e = 2.6$, $Re_u = 4.9$ mio/m

sandpaper. Right downstream of the sandpaper, high surface temperatures indicate a turbulent boundary layer. In the region downstream of the blowing holes, the temperature is decreased due to the cooling gas. Boundary layer tripping and cooling both appear uniform over the length of the model / the perforated area.

During the experiments, temperature histories are recorded by means of thermocouples. From the temperature signals, heat fluxes are deduced. In order to calculate the cooling efficiency, reference experiments without cooling are needed. Those are performed after a series of experiments with the blowing slot being filled with glue to avoid steps and cavities which can cause flow disturbances. Fig. 4 shows the heat fluxes from those reference experiments without blowing for all experimental conditions tested in this report. Measured values scatter around theoretical curves calculated with semi-empirical equations by Simeonides [9]. Part of the scatter can be explained by different sensitivities of the thermocouples, wich cancels out when the cooling efficiency is calculated. It can be seen, that turbulent heat fluxes exceed the laminar ones, as expected. Their large difference leaves no doubt, that triggering of the boundary layer in the case of turbulent flow is successful. Because the Mach number is adjusted by the inclination of the model, thus, the strength of its front shock, lower Mach numbers behind the shock lead to higher heat fluxes, due to increased static temperature of the flow. For the Mach numbers 4.9, 2.6 and 1.5, static temperatures amount to 230 K, 510 K and 810 K.
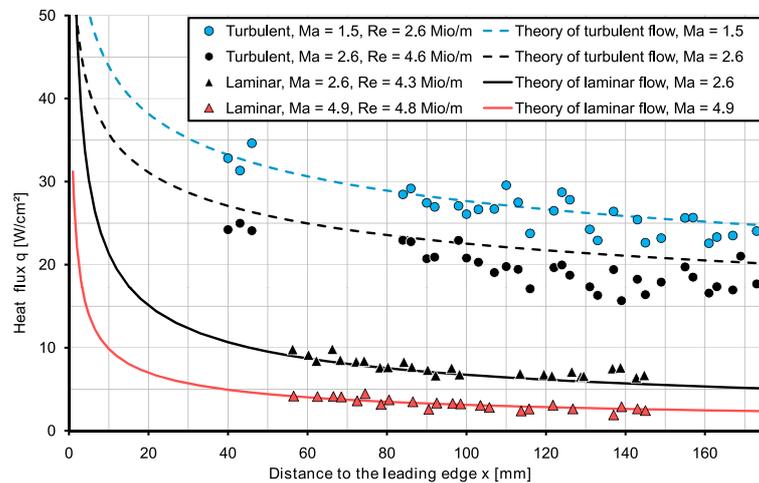

Figure 4: Reference experiments without cooling gas injection and theoretical values calculated with semi-empirical equations from Simeonides [9].

4. Experimental results

To demonstrate the effect of different main stream conditions, experiments with the same blowing ratio in turbulent boundary layer flows with different Mach numbers have been compared, Fig. 5. As described in chapter 3, Reynolds numbers changed as well. Heat fluxes for the lower Mach number condition Ma= 1.5, Re_u = 3.0 mio/m are higher than those for Ma= 2.6 and Re= 4.9 mio/m. Since reference heat fluxes are higher as well, this effect cancels out when calculating the cooling efficiency according to Eq. (2). Using the correlation function Eq. (5) will shift the values to make them fit to one curve, especially in the part of low distances to the slot exit. Fig. 6 shows correlated data of experiments with different blowing ratios and Mach numbers, with the previously shown experiments for the Mach number comparison marked as triangles. A logarithmic scale has been chosen to emphasize the region of low correlation parameters, where the cooling efficiency is high. In this region cooling efficiency drops fast and high gradients occur, thus, an enlarged scale helps reading the data in this region. Because correlated results show no difference anymore, the influence of the Mach number is represented by the corresponding factor used by the correlation function. For the case of $Ma = 1.5$ we obtained $C^* = 1.10$, $T_e/T^* = 1.28$ and Re_u = 3.0 mio/m. This gives a factor of $(C^*/Re_u)^{0.2}(T_e/T^*)^{0.6} = 0.060m^{0.2}$. For the case of $Ma = 2.6$ we get a factor of $(C^*/Re_u)^{0.2}(T_e/T^*)^{0.6} = 0.044m^{0.2}$ for $C^* = 0.98$, $T_e/T^* = 0.95$ and Re_u = 4.9 mio/m. When the same cooling efficiency is reached with an identical correlation parameter at different Mach numbers but for the same blowing ratio, the running length must be different. Since the $(C^*/Re_u)^{0.2}(T_e/T^*)^{0.6}$ factor is for Mach 2.6 flow 0.74 times as high as for the Mach 1.5 flow, $x'^{0.8}$ must

compensate for that with x' beeing 1.45 times higher in the case of the higher Mach number. This implies that the cooling effect will extend further downstream for the combined effect of higher Mach and Reynolds numbers, as shown in Fig. 5.
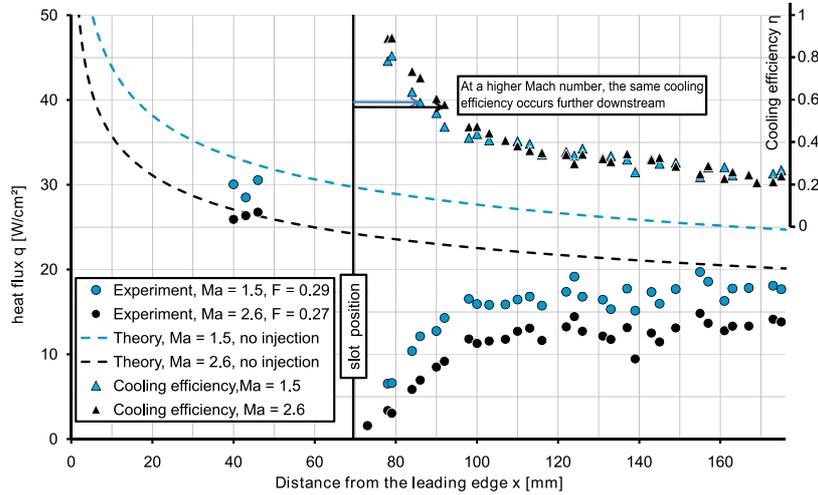

Figure 5: Heat fluxes of experiments at different main stream Mach numbers and their cooling efficiency in turbulent flow.
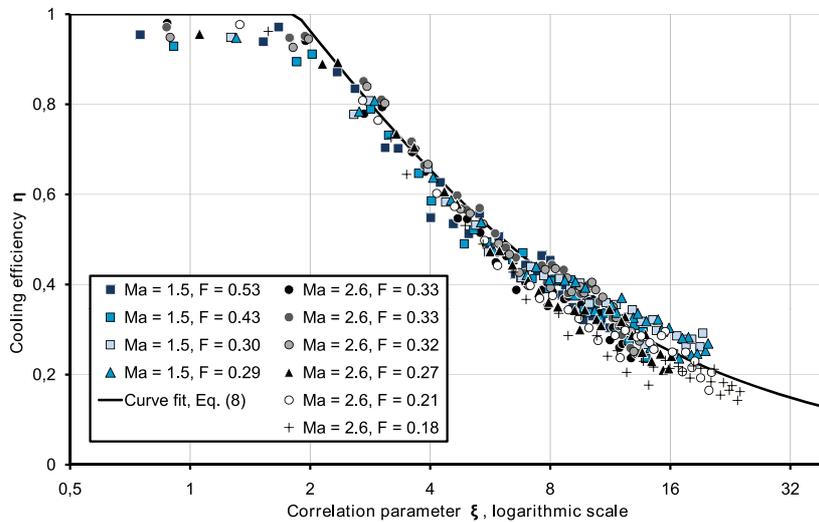

Figure 6: Cooling efficiency of air injection at different blowing ratios and Mach numbers for turbulent flow.

Film cooling in turbulent flows has been numerically simulated previously by Martelli et al., as mentioned in chapter 2. Although the flow Mach and Reynolds number are different, a correlation similar to Eq. (5) is applied and a curve fit is used, Eq. (9). However, in contrast to this work Martelli's correlation doesen't contain the previously mentioned flow condition factor $(C^*/Re_u)^{0.2}(T_e/T^*)^{0.6}$, and scales with x' rather than $x'^{0.8}$. Fig. 7 shows results of the rocket nozzle simulations [1]. In order to compare the correlation used, the flow condition factor has been calculated for Martelli's flow. Since an adiabatic wall is simulated there, the wall temperature changes with the distance from the blowing opening. At the slot exit, the wall reaches coolant temperature and a cooling efficiency of 1, whereas far downstream the wall reaches recovery temperature and $\eta = 0$. Because the wall temperature is a part of the reference temperature T^*, which also appears in the Chapman-Rubesin factor C^*, the flow condition factor starts at 0.032 and changes continuously till it reaches 0.050. Another problem are changing flow properties due to expanding flow (not

incorporated in the flow condition factor for $\eta = 0$, because the running length of coolant film breaking varies with the blowing ratio). Therefore, cooling efficiency is compared in the vicinity of the blowing opening, where high blowing ratios are present and $(C^*/\mathrm{Re}_u)^{0.2}(T_e/T^*)^{0.6} = 0.032$ is assumed being constant. Because this factor is missing in Martelli's correlation, his correlation parameter has been multiplied with 0.032 before inserting it into the curve fit of this paper, Eq. (8). The only difference left is the slightly different running length parameter, x' instead of $x'^{0.8}$. The resulting curve can be plotted next to the data of [1] and has been added to Fig. 7. The comparison shows, that the point where cooling efficiency starts to drop matches pretty well, maybe due to the assumption of $\eta \approx 1$ for the flow condition factor still beeing valid at this point. The decrease itself is predicted to be more rapidly by the curve fit proposed by this paper. The reason for this could be the expansion of the nozzle flow, delivering higher cooling efficiencies for higher Mach numbers, just like the shock compressed flow of this work does. Thus, higher cooling efficiencies than expected occur at positions further downstream, where the Mach number is higher than the Mach number at the blowing exit.
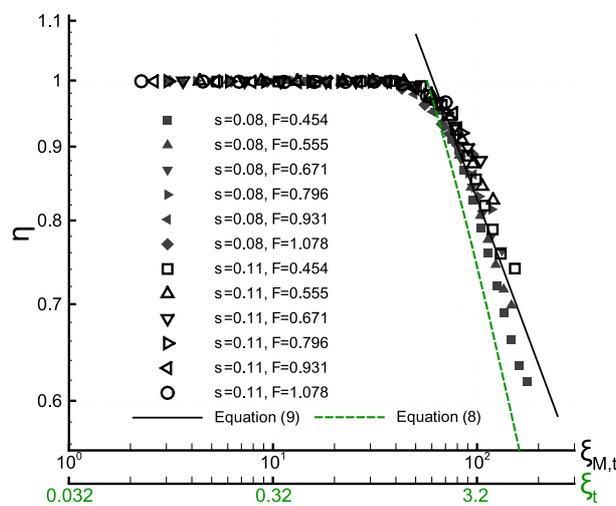

Figure 7: Cooling efficiency of rocket nozzle cooling at $Ma_e = 3.65$ by Martelli et al. [1]. Labels changed and curve fit Eq. (8) added. In this case s is the slot height divided by the throat radius, giving a nondimensional value.

Whilst the agreement of correlated results for slotted film cooling experiments is quite good, investigations with two rows of 45° inclined blowing holes show a lower cooling efficiency for both Mach numbers tested, as shown in Fig. 8. As mentioned by Linn and Kloker [13], a complex vortex structure is formed around blowing holes, leading to enhanced mixing with the turbulent boundary layer. This leads to a faster heating of the coolant and lower cooling efficiencies. Furthermore the inclination angle of the holes of 45° compared to 10° for the inclined slot and the smaller slot width of 1 mm compared to 1.7 mm causes a higher blowing impulse perpendicular to the wall which leads to enhanced mixing of the flow.

Cooling in laminar boundary layer flow has ben investigated for different blowing ratios and Mach numbers as well [14]. For laminar flow a different correlation is used, Eq. (4), as the laminar boundary equations show different behavior than the turbulent ones. The dependencies of the cooling efficiency can be expressed by the factors contained in the correlation parameter, like in turbulent flows, so correlated data follows one curve, approximated by a curve fit for laminar film cooling Eq. (7). Correlated data is shown in Fig. 9 along with the curve fit. Experiments with different cooling gases showed that light gases lead to a high cooling efficiency. This has also been observed for Helium by Gülhan and Braun in experiments with transpiration cooling through porous media [15]. They believe that the seven times higher volume flow of Helium when injecting at the same blowing ratio is the reason for the significantly better cooling behavior. A cooling gas factor, Eq. (6), has been employed to correlate data of experiments with different cooling gases, meaning that the influence of gas properties is represented by this factor rather than by the correlated plots, see Fig. 10.
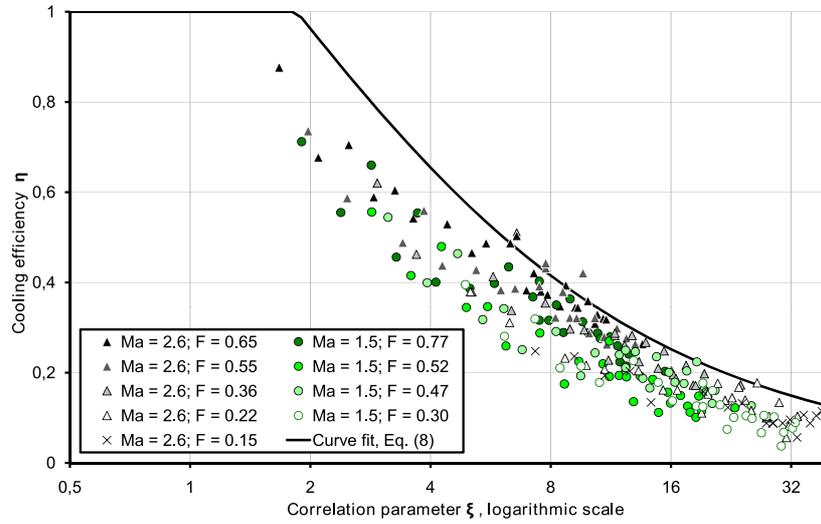
Figure 8: Cooling efficiency of air injection with two rows of inclined blowing holes at Mach numbers 2.6 and 1.5 in turbulent flow.
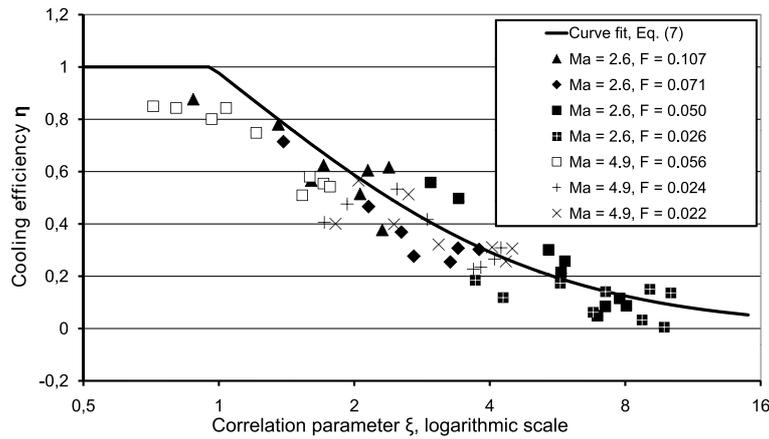

Figure 9: Mach number influence of the cooling efficiency for a flat plate in laminar Mach 2.6 and Mach 4.9 flow with air injection.
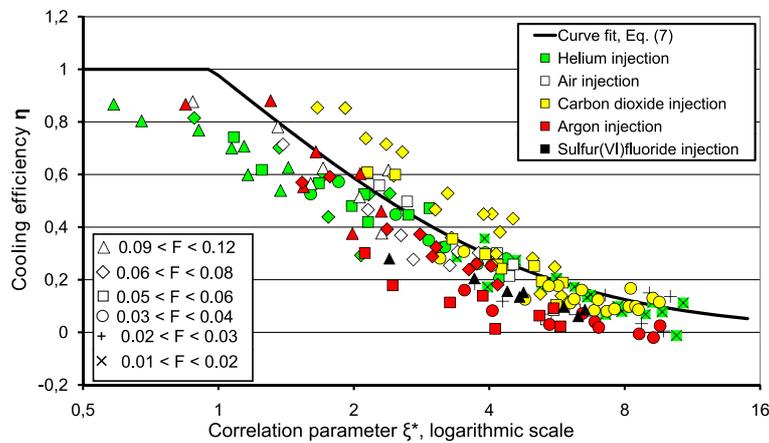

Figure 10: Cooling efficiency of different coolant gases, correlated using a coolant gas factor.

5. Conclusion

Film cooling experiments at a flat plate supported by a wedge model have been conducted for various experimental setups. From previous works, the dependency of the coolant mass flow $F \times s$ on the cooling efficiency is well known and a higher mass flow provides higher cooling efficiencies, for both turbulent and laminar flow. A variation of the main flow Mach number by changing the preceeding shock compression showed, that higher Mach numbers lead to higher cooling efficiencies, for both flow regimes. Investigations with two rows of blowing holes in turbulent flow delivered lower cooling efficiencies than for slotted blowing at the same conditions. An investigation of different cooling gases has been conducted for laminar flow, and a cooling gas factor is proposed. The described dependencies of the film cooling efficiency have been incorporated in two correlation functions, a laminar one and another for turbulent flow. The factors of the correlation functions describe the dependencies of the film cooling efficiency on various parameters whereas correlated cooling efficiencies cluster around one curve. However, not all parameters are yet incorporated in the correlation. Injection through blowing holes, for instance, shows lower cooling efficiencies than predicted. This report is ment to be another step to understanding of the physical effects that take place in film cooling, with the goal to improve future applications such as rocket nozzle cooling. Further research will focus on tangential film cooling and the influence of the blowing angle on the cooling efficiency.

References

[1] Martelli, E., Nasuti, F. and Onofri, M. 2009. Numerical analysis of film cooling in advanced rocket nozzles. *AIAA Journal* 47/11: 2558–2566.

[2] Keener, D., Lenertz, J., Bowersox, R. and Bowman, J. 1995. Transpiration cooling effects on nozzle heat transfer and performance. *J. of Spacecraft and Rockets* 32/6:981–985.

[3] Yang, X., Badcock, K. J. and Richards, B. E. 2003. A numerical study of hypersonic laminar film cooling. *Aeronautical Journal* 107/1074:479–486.

[4] Richards, B. E. 1967. Film cooling in hypersonic flow. *PhD thesis, University of London.*

[5] Holden, M. S. and Rodriguez, K. 1994. Experimental studies of shock-wave / wall-jet interaction in hypersonic flow. *NASA-CR-195844*

[6] Goldstein, R. J. 1971. Film cooling. *Advances in Heat Transfer* 7:321–379.

[7] Heufer, K. A. and Olivier, H. 2008. Experimental and numerical study of cooling gas injection in laminar supersonic flow. *AIAA Journal* 46/11:2741–2751.

[8] Eckert, E. R. G. 1955. Engineering relations of friction and heat transfer to surfaces in high velocity flows. *J. of Aeronautical Sciences* 22/8:585–587.

[9] Simeonides, G. 1995. Simple theoretical and semi-empirical convective heat transfer predictions for generic aerodynamic surfaces. *ESA Propulsion and Aerothermodynamics Division, Technical report YPA/1576/GS*

[10] Sahoo, N., Kulkarni, V., Saravanan, G., Jagadeesh, G. and Reddy, K. P. J. 2005. Film cooling effectiveness on a large angle blunt cone flying at hypersonic speed. *Physics of Fluids* 17/3:036102.

[11] Gröning, H. and Olivier, H. 1998. Experimental hypersonic flow research in Europe. *JSME International J. Series B* 41/2:397–407.

[12] Olivier, H., Jiang, Z., Yu, H. R. and Lu, F. 2002. Detonation driven shock tubes and tunnels. *Progress in Astronautics and Aeronautics, AIAA Inc.* 198:135–203.

[13] Linn, J. and Kloker, M. J. 2010. Effects of wall-temperature conditions on effusion cooling in a supersonic boundary layer. *AIAA Journal* 49/2:299–307.

[14] Hombsch, M. and Olivier, H. 2010. Flow condition and cooling gas variation for film cooling studies in hypersonic flow. *SFB / TRR40 Annual Report 2010, München* 27–39.

[15] Gülhan, A. and Braun, S. 2010. An experimental study on the efficiency of transpiration cooling in laminar and turbulent hypersonic flows. *Experiments in Fluids* 50/3:509–525.